Lattice Engineering in MnO_2 via V^{5+} Doping for High-Performance Aqueous Te–MnO_2 Batteries

Xinyang Zhang [a], Xiaoyu Yang [a], Yingjun Wei [a], Dewei Wang [a,*], Yuhong Chen [b]

[a] College of Materials Science and Engineering, North Minzu University, Yinchuan 750021, People's Republic of China. Email: wangdewei@yeah.net (D. Wang)

[b] Key Laboratory of Powder Material and Advanced Ceramics, Yinchuan 750021, People's Republic of China.

Computational details

All spin-polarized density functional theory (DFT) computations were carried out using the Vienna Ab initio Simulation Package (VASP). The Perdew–Burke–Ernzerhof (PBE) functional within the generalized gradient approximation (GGA) was employed to represent the exchange–correlation interactions. Electron–ion interactions were treated using the projector augmented wave (PAW) method. A plane-wave energy cutoff of 450 eV was applied, and Brillouin zone sampling was performed with a 2×9×6 Monkhorst–Pack k-point grid. The convergence thresholds for the self-consistent field iterations were set to 10^{-5} eV for energy and 0.02 eV $Å^{-1}$ for forces. To better describe the strongly correlated electrons, the DFT+U approach was applied with effective U values of 5.5 eV for Mn and 4.0 eV for V. Van der Waals interactions were incorporated via the DFT-D3 correction scheme. Structural models and calculation results were visualized using VESTA.

Preparation of α-MnO_2

A solution of $KMnO_4$ (0.395 g, 0.008 mol) in deionized water (35 mL) was mixed with $MnSO_4 \cdot H_2O$ (0.169 g). The mixture was stirred magnetically for 30 minutes. It was then transferred into a Teflon-lined stainless-steel autoclave and heated at 160 °C for 12 hours. The resulting solid product was collected, washed repeatedly with deionized water and ethanol, and dried overnight at 60 °C.

Preparation of β-MnO_2

$MnSO_4 \cdot H_2O$ (1.352 g, 0.008 mol) and $(NH_4)_2S_2O_8$ (1.826 g, 0.008 mol) were dissolved in deionized water (40 mL) under magnetic stirring. After 30 minutes, the mixture was transferred into a Teflon-lined stainless-steel autoclave and heated at 140 °C for 12 hours. The solid product was washed several times with deionized water and ethanol, and then dried at 60 °C overnight.

Preparation of γ-MnO_2

$MnSO_4$ (4.50 mmol) was dissolved in deionized water, followed by the addition of an aqueous $(NH_4)_2S_2O_8$ solution (4.93 mmol). The mixture was placed in a Teflon-lined stainless-steel autoclave and heated at 90 °C for 24 hours. The solid product was washed multiple times with deionized water and ethanol, and finally dried at 60 °C overnight.

Synthesis of C@Te composite

100 mg of tellurium powder was thoroughly mixed with 50 mg of Ketjen black, then transferred to a tube furnace and heated to 500 °C at a rate of 2 °C min^{-1} under an argon atmosphere, followed by maintaining at that temperature for 5 h.

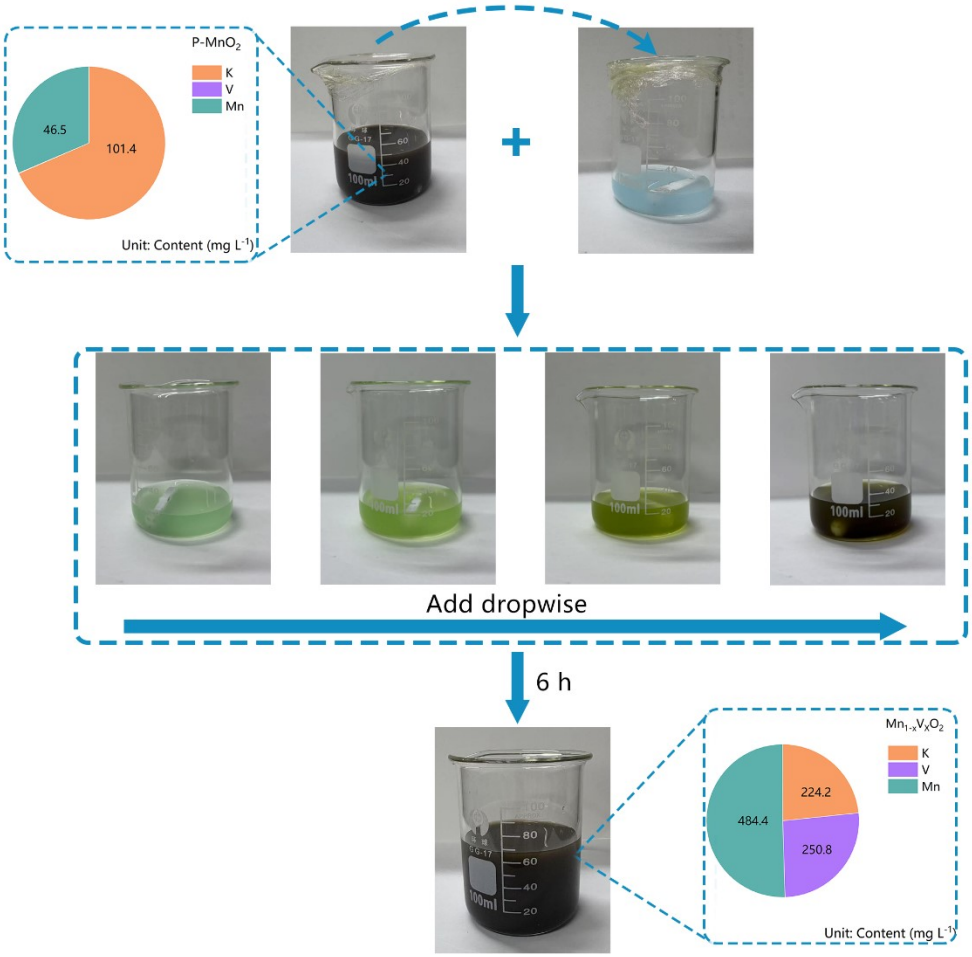

Figure S1. Schematic diagram of the reaction process, showing the elemental composition and content before and after the reaction.

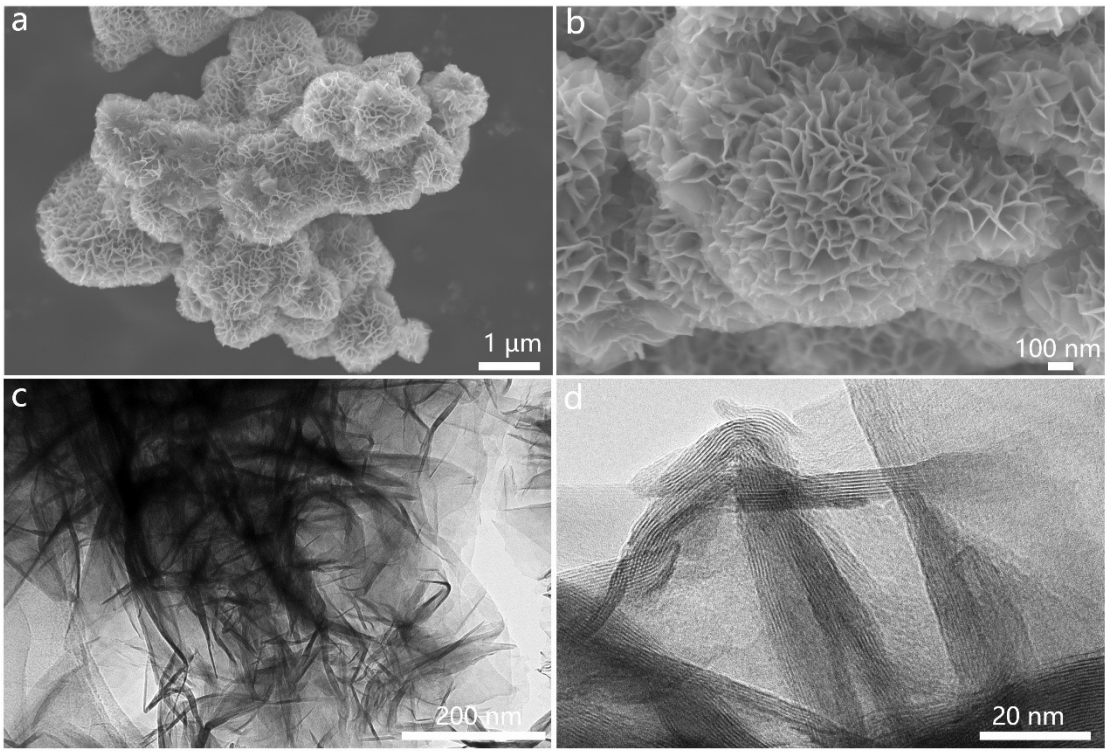

Figure S2. (a, b) SEM and TEM (c, d) images of P-MnO_2 at different magnifications.

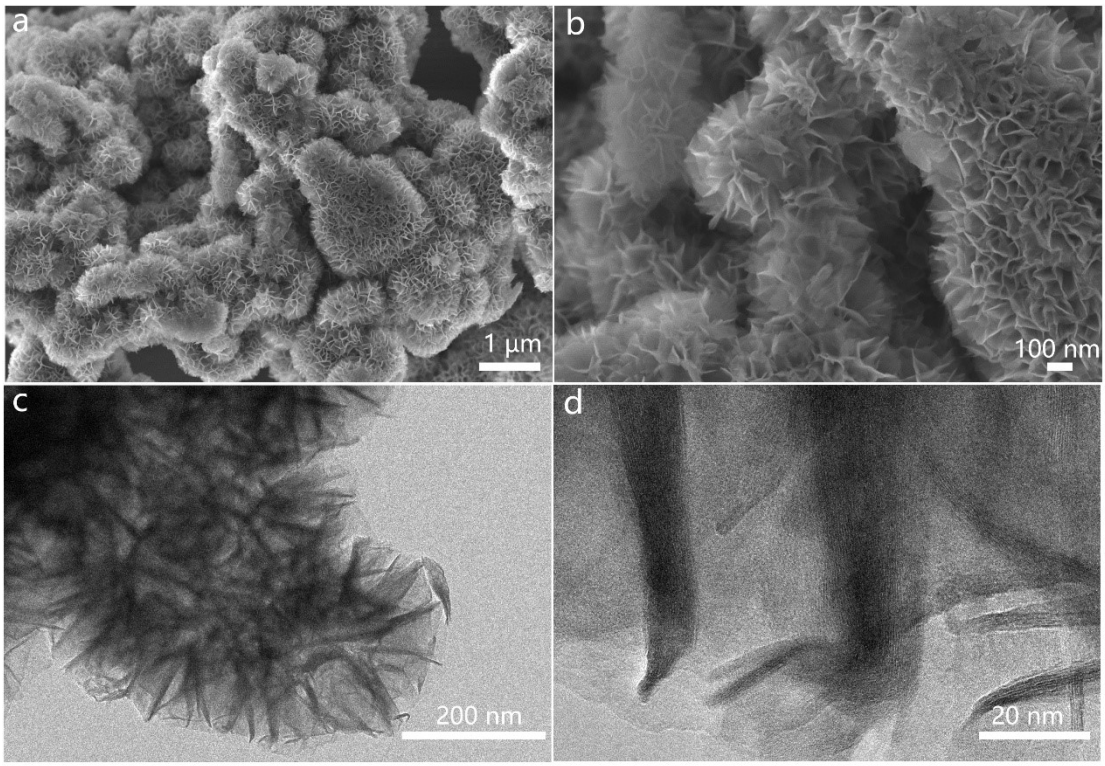

Figure S3. (a, b) SEM and TEM (c, d) images of $Mn_{1-x}V_xO_2$ at different magnifications.

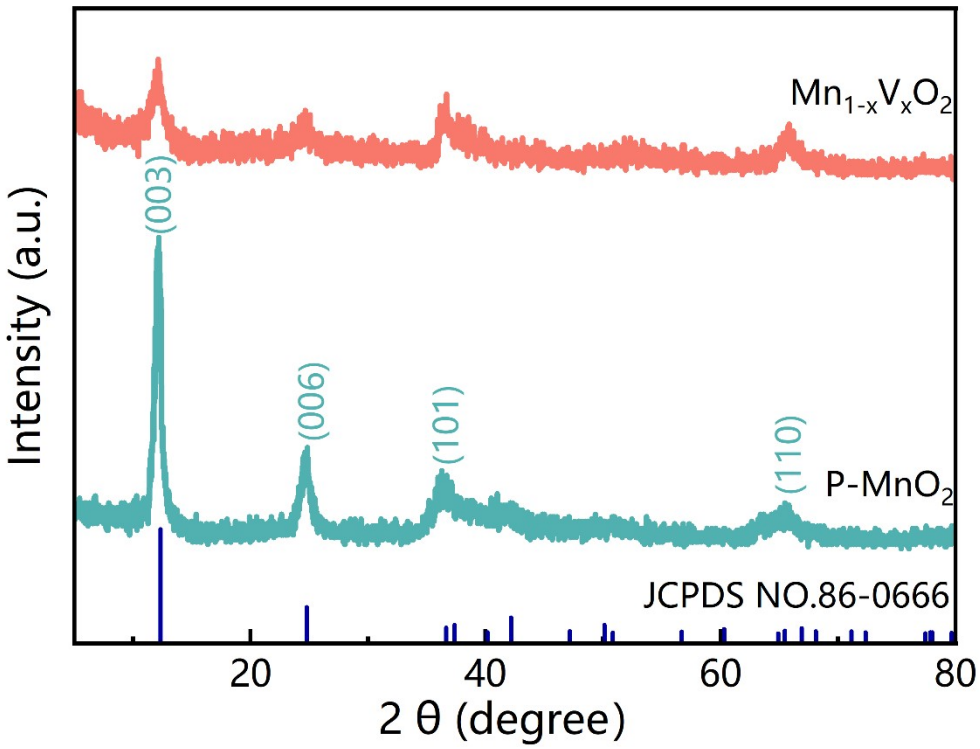

Figure S4. XRD pattern of the samples.

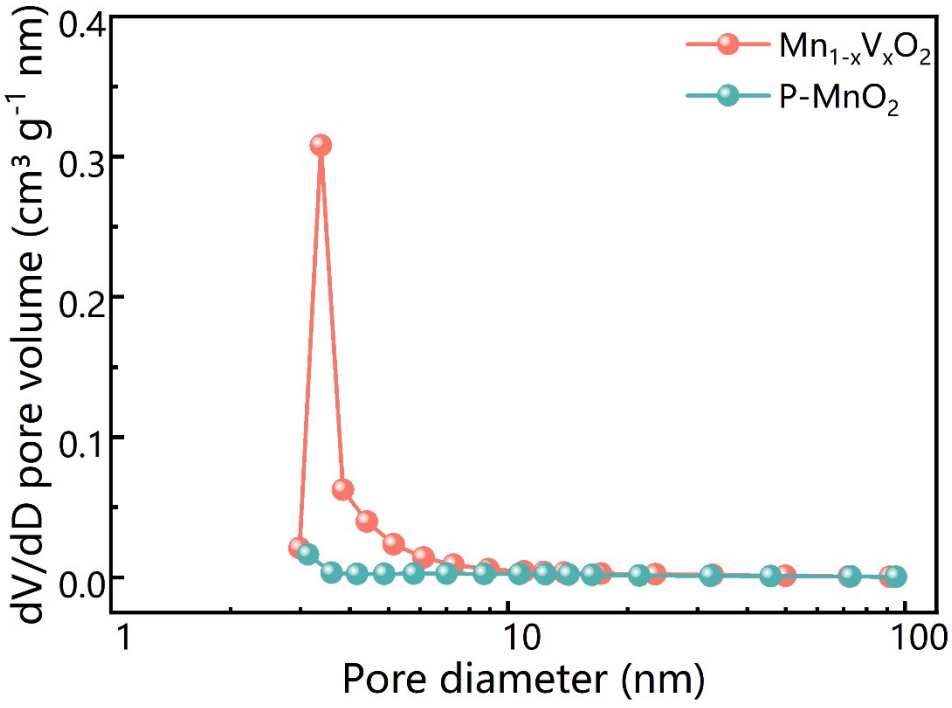

Figure S5. Pore size distribution curves of the samples.

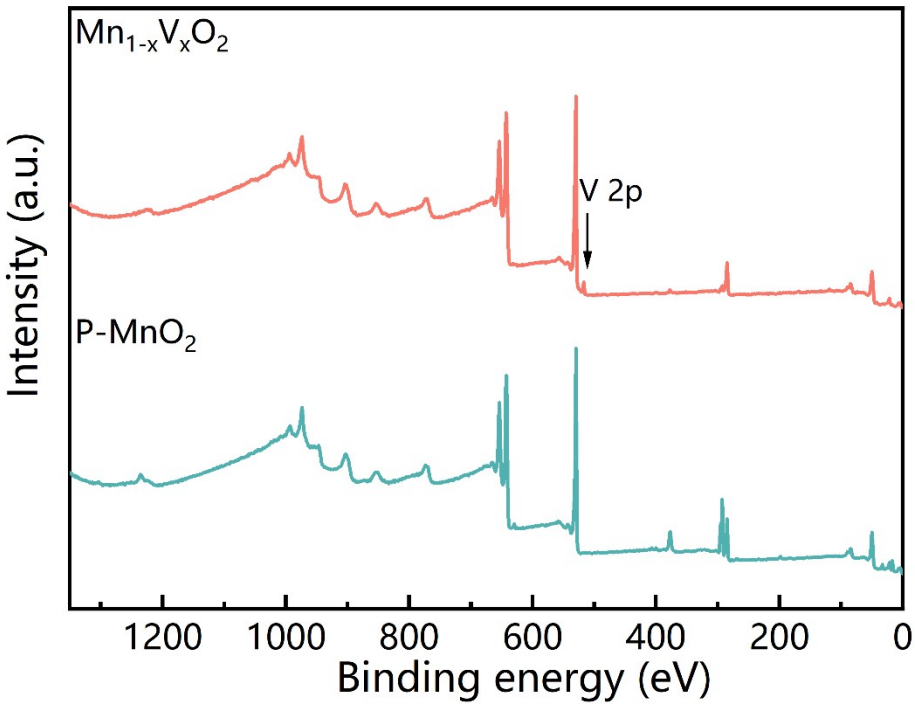

Figure S6. XPS survey spectrum of the samples.

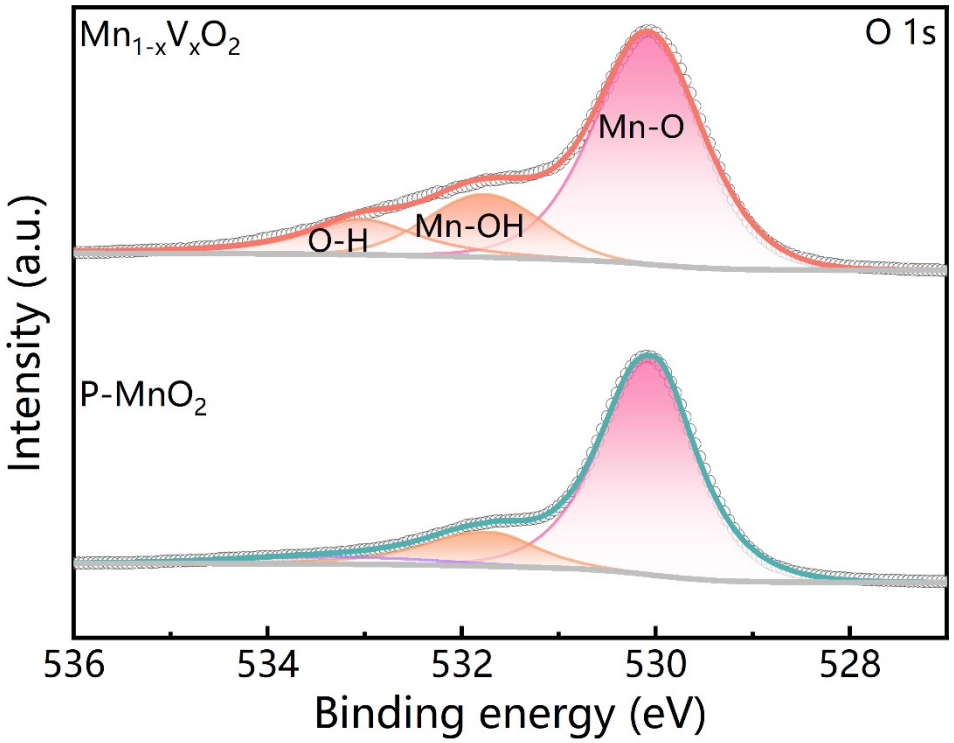

Figure S7. High-resolution XPS spectrum of O 1s.

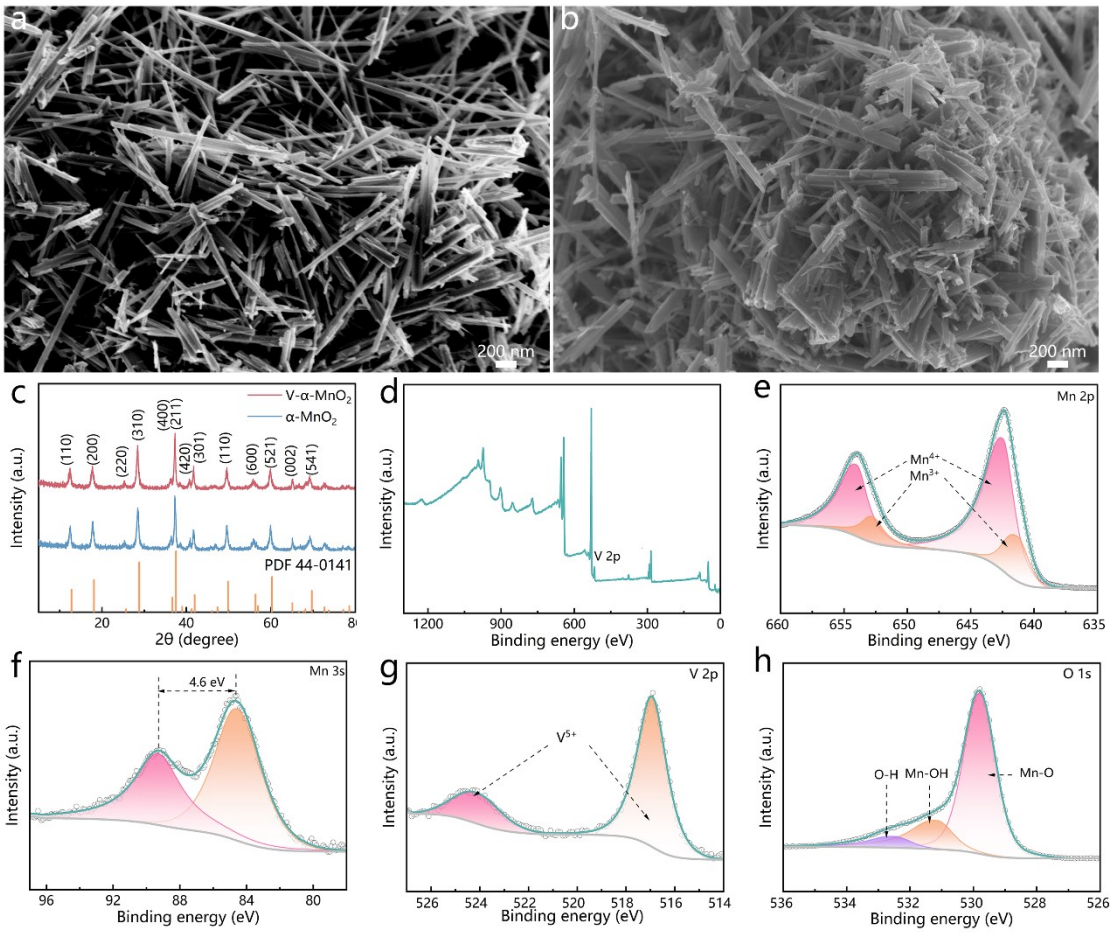

Figure S8. Morphological and structural characterization: (a) Pristine α-MnO_2 before reaction, (b) V-doped α-MnO_2, (c) XRD patterns, (d) XPS survey spectrum of V-doped α-MnO_2, and (e-h) high-resolution XPS spectra of (e) Mn 2p, (f) Mn 3s, (g) V 2p, and (h) O 1s.

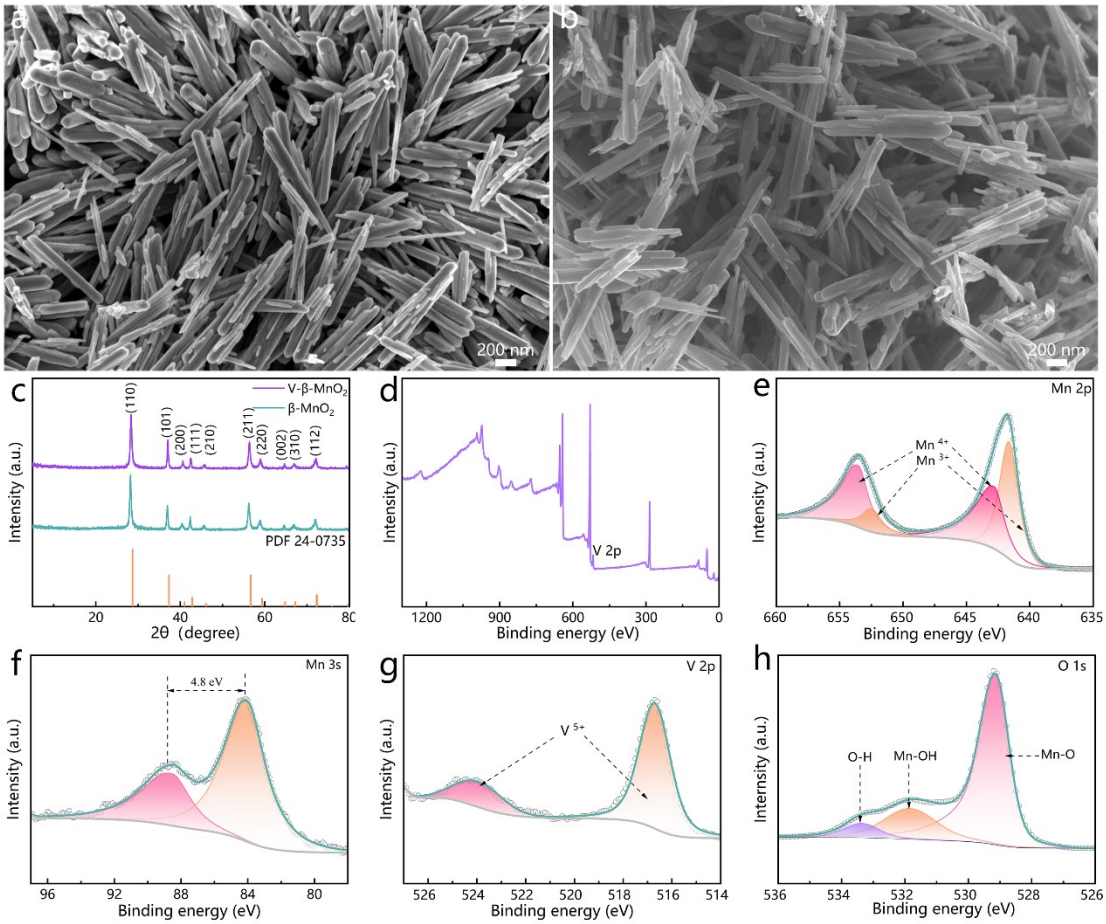

Figure S9. Morphological and structural characterization: (a) Pristine β-MnO_2 before reaction, (b) V-doped β-MnO_2, (c) XRD patterns, (d) XPS survey spectrum of V-doped β-MnO_2, and (e-h) high-resolution XPS spectra of (e) Mn 2p, (f) Mn 3s, (g) V 2p, and (h) O 1s.

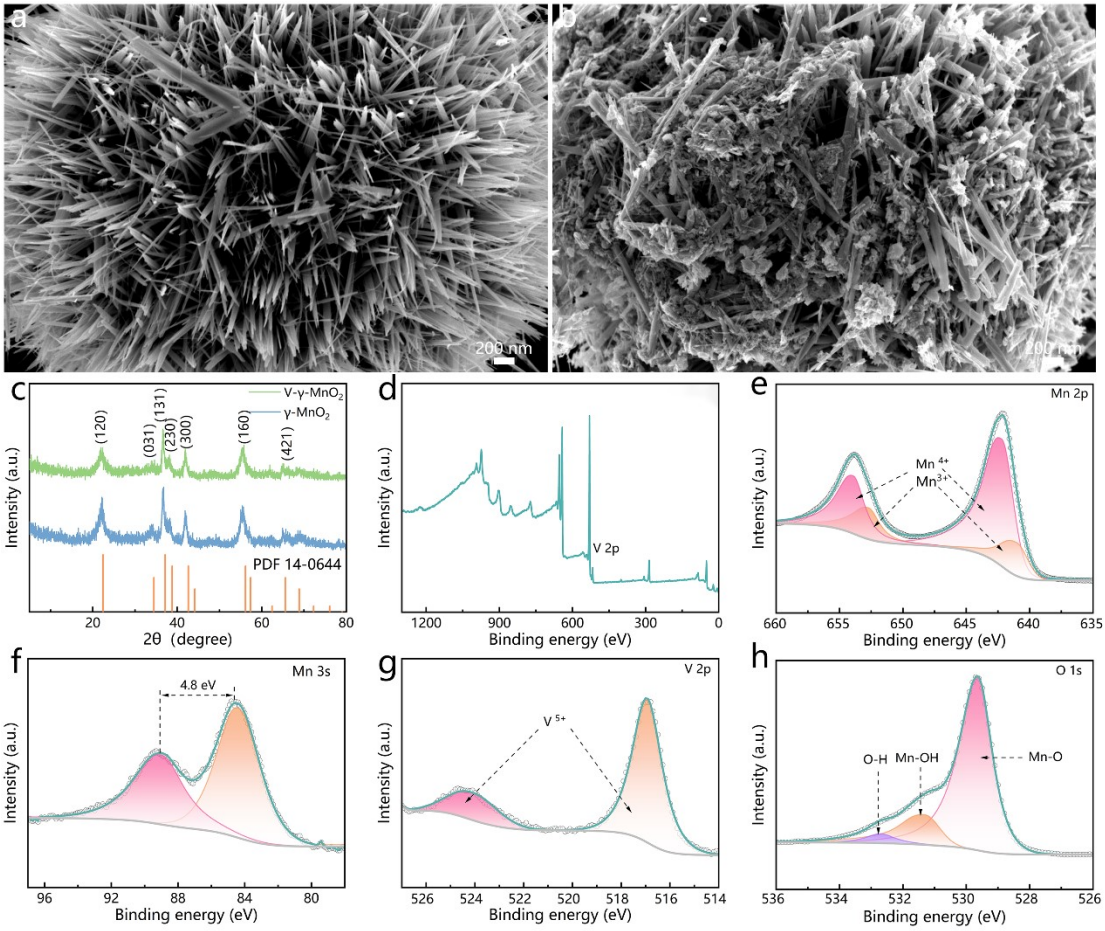

Figure S10. Morphological and structural characterization: (a) Pristine γ-MnO_2 before reaction, (b) V-doped γ-MnO_2, (c) XRD patterns, (d) XPS survey spectrum of V-doped γ-MnO_2, and (e-h) high-resolution XPS spectra of (e) Mn 2p, (f) Mn 3s, (g) V 2p, and (h) O 1s.

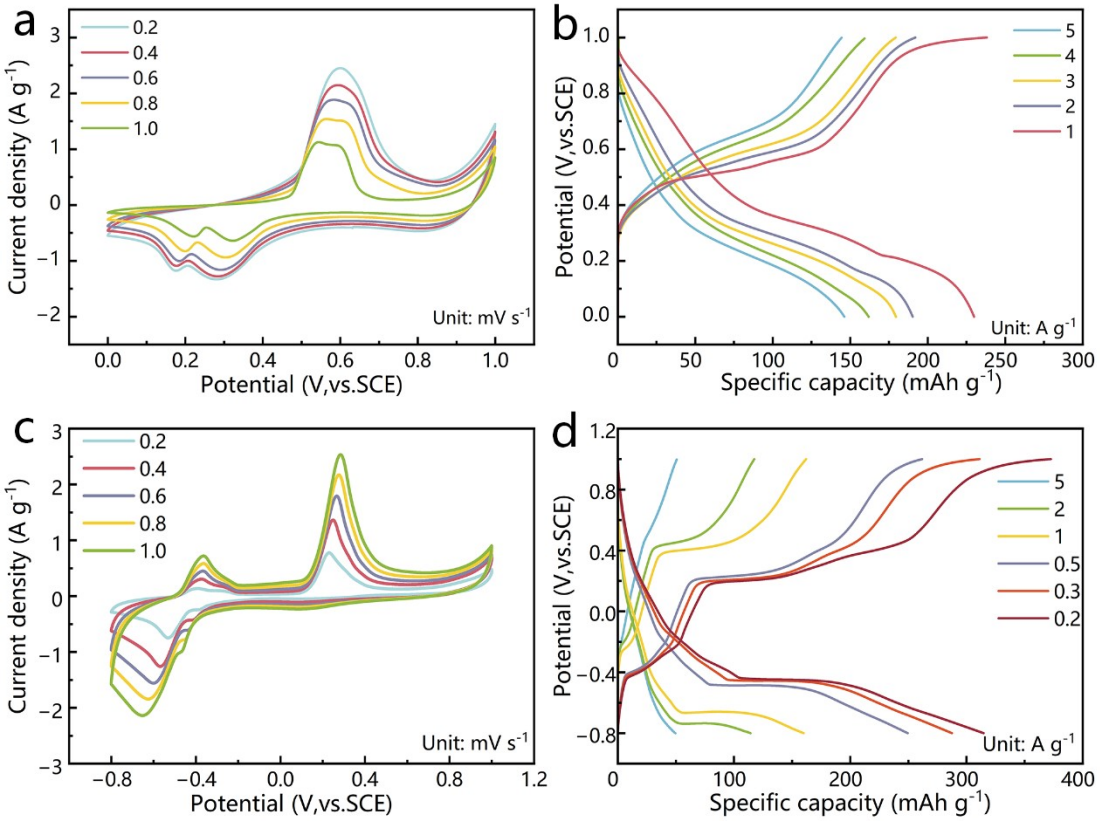

Figure S11. Electrochemical performance of the $Mn_{1-x}V_xO_2$ and C@Te in three-electrode configuration. (a) CV curves and (b) GCD curves of the $Mn_{1-x}V_xO_2$; (c) CV curves and (d) GCD curves of the C@Te.

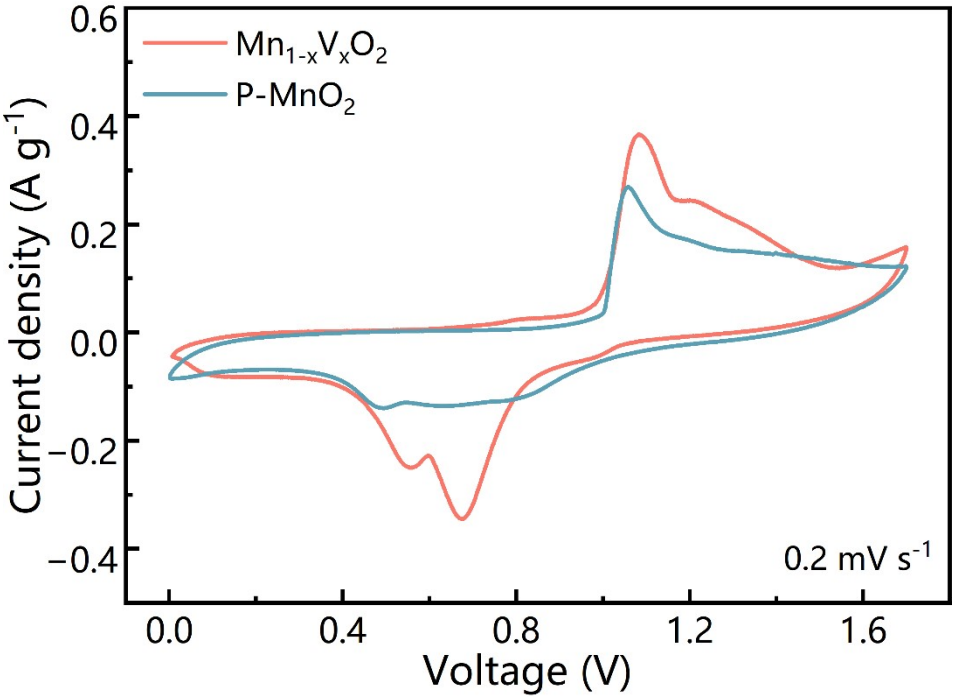

Figure S12. CV curves of the samples.

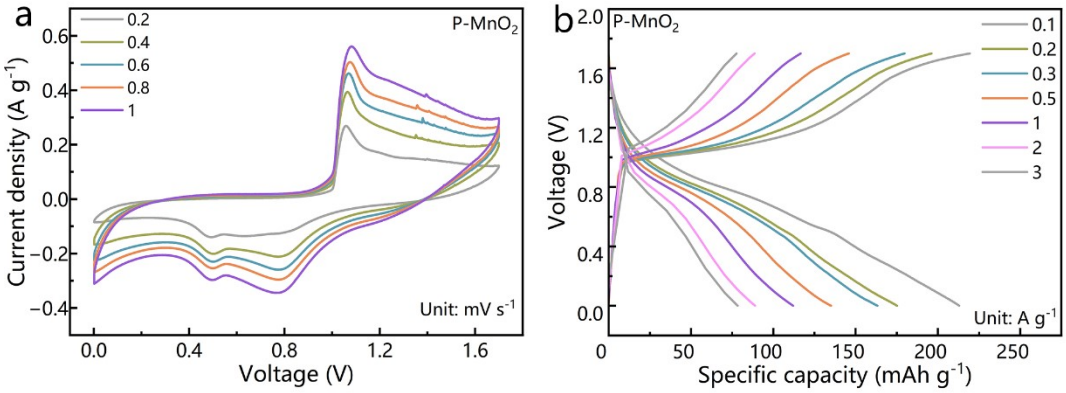

Figure S13. CV and GCD curves of the P-MnO_2.

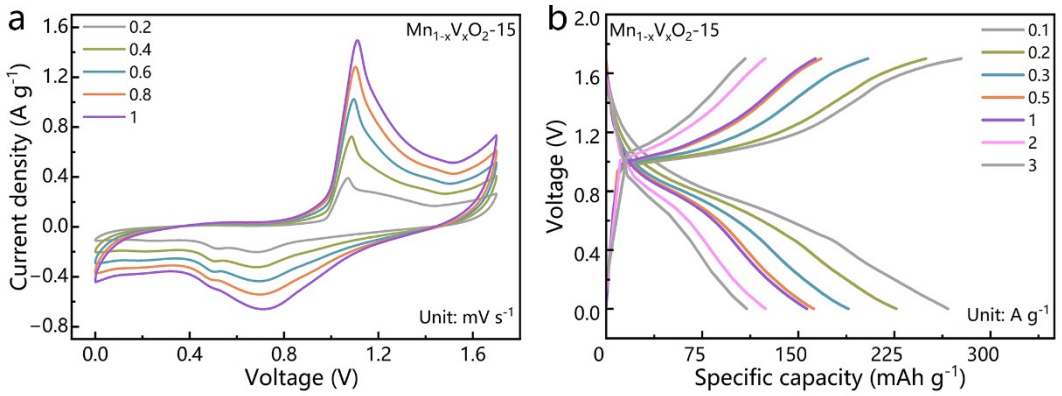

Figure S14. CV and GCD curves of the samples obtained at the low content of $VOSO_4$ (15 mg).

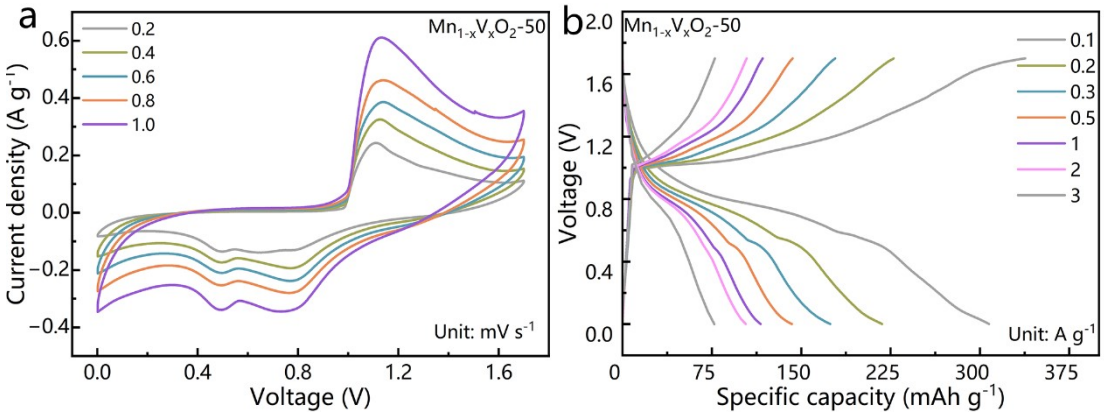

Figure S15. CV and GCD curves of the samples obtained at the high content of $VOSO_4$ (50 mg).

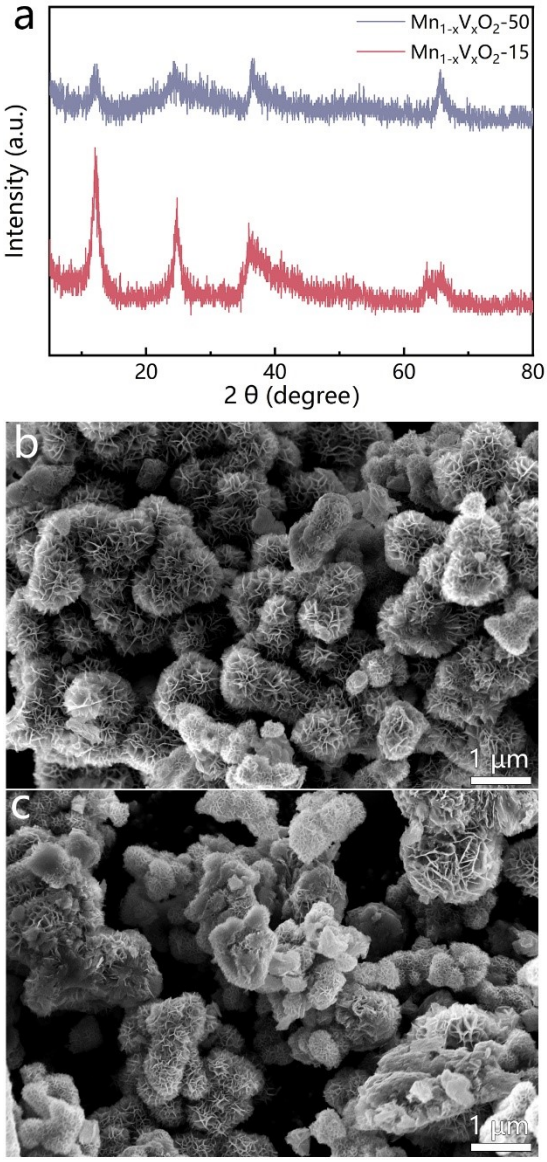

Figure S16. (a) XRD patterns of the samples obtained from low (15 mg) and high (50 mg) $VOSO_4$ content. SEM image of the (b) low (15 mg) and (c) high (50 mg) $VOSO_4$ content.

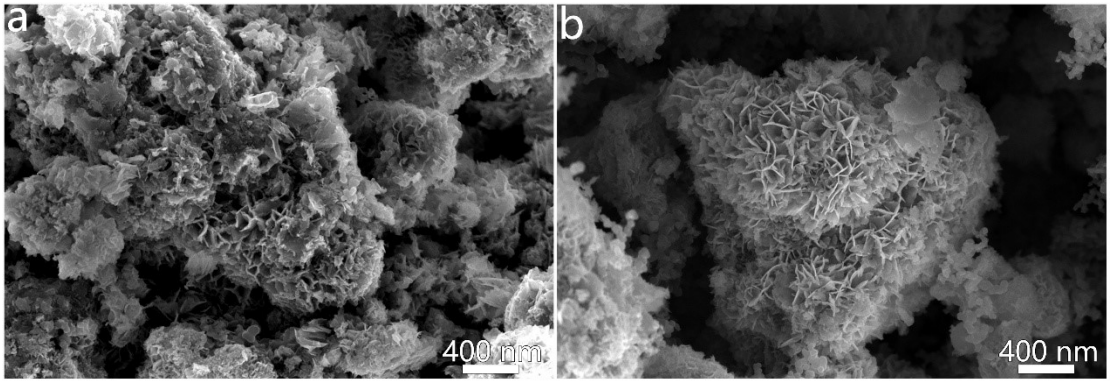

Figure S17. SEM images after cycling test, (a) P-MnO_2 and (b) $Mn_{1-x}V_xO_2$.

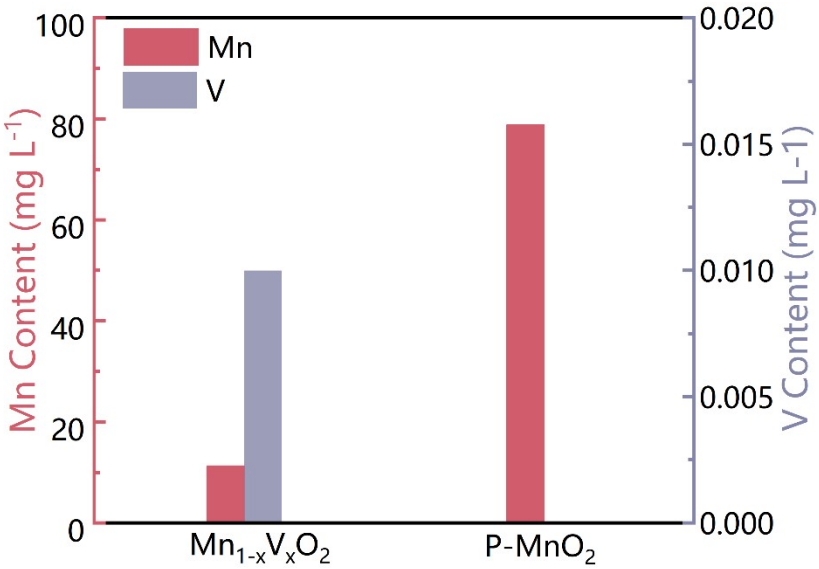

Figure S18. The content of Mn and V in the electrolyte after the cycle stability test.

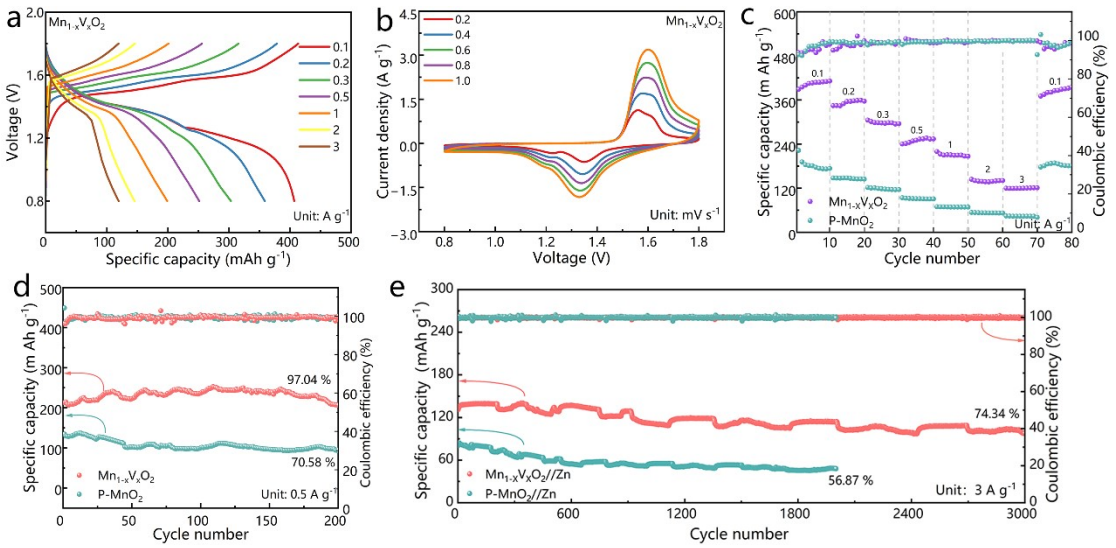

Figure S19. Electrochemical performance of the Zn-MnO_2 battery. (a, b) GCD and CV curves of the $Mn_{1-x}V_xO_2$ cathode. (c) Rate capability. (d, e) Cycling stability at 0.5 and 3 A g^{-1}, respectively.

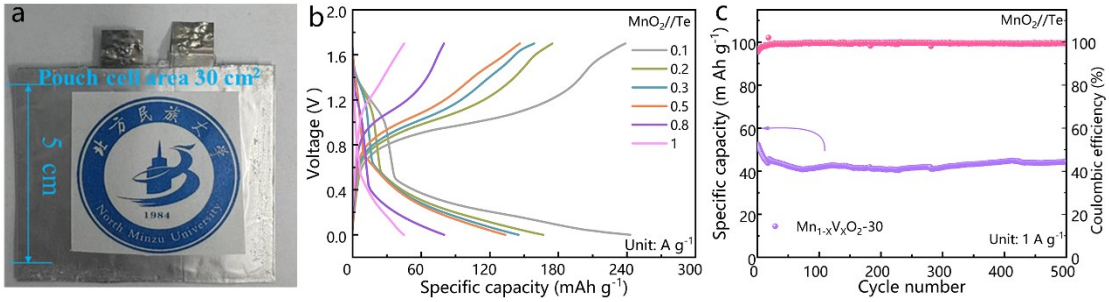

Figure 20. Electrochemical performance of pouch cell: (a) Photograph, (b) GCD profiles, and (c) cycling stability at 1 A g^{-1}.

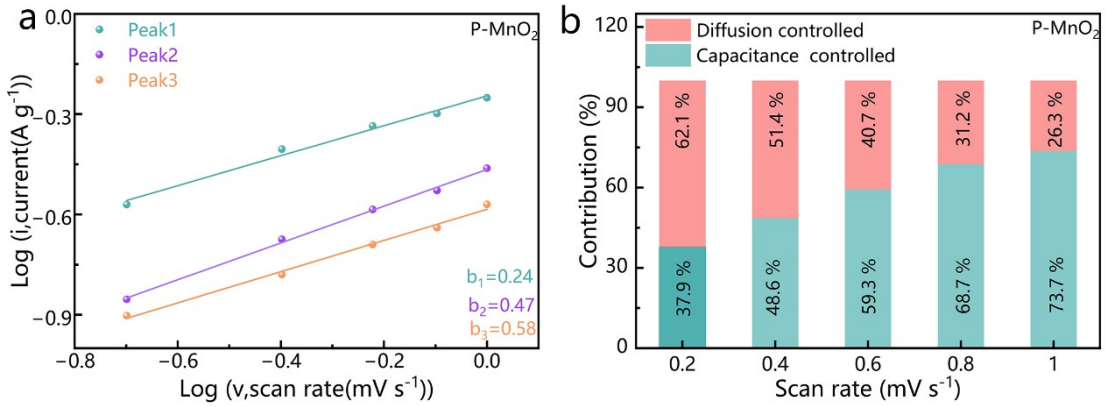

Figure S21. (a) Relationship between log(i) and log(v). (b) Contribution ratio of capacitive and diffusion-controlled capacities at different scan rates for P-MnO_2.

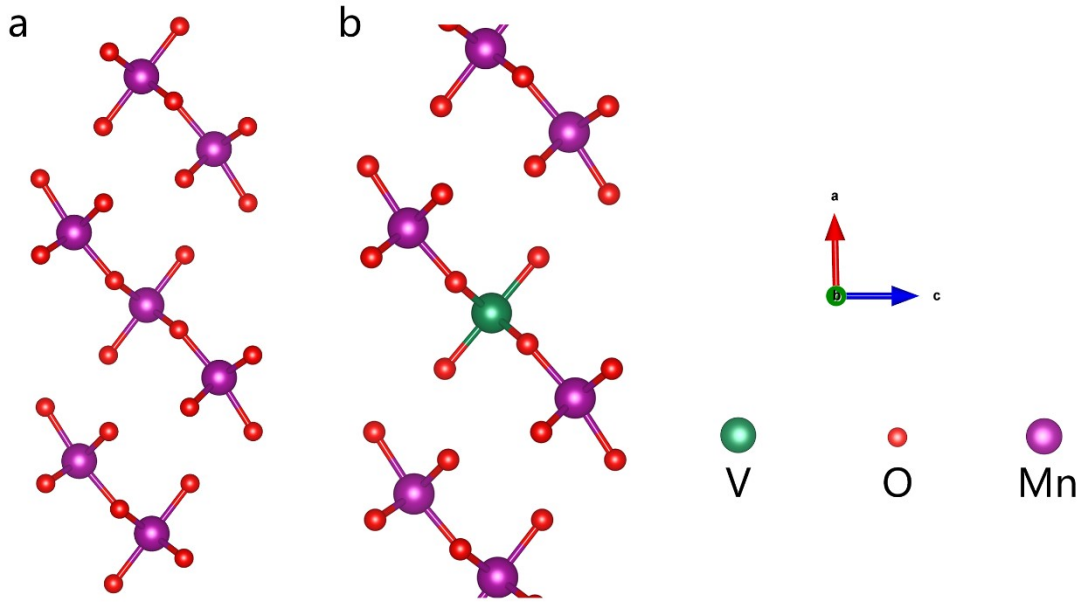

Figure S22. Crystal structures of (a) P-MnO_2 and (b)V-doped MnO_2.

Table S1. Refined fractional atomic coordinates and their estimated standard deviations.

sample	P-MnO2			$Mn_{1-x}V_xO_2$		
atom	x	y	z	x	y	z
Mn0	0.14624	1/2	0.01621	0.15931	1/2	0.02027
Mn1	0	0	1/2	0	0	1/2
O2	0.04354	1/2	0.17379	0.06114	1/2	0.30635
O3	0.12784	0	0.42584	0.10068	0	0.79902
O4	0.31993	0	0.55043	0.22602	0	0.21585
V				0.15931	1/2	0.02027
V				0	0	1/2

Table S2. Comparison of the electrochemical performance of the $Mn_{1-x}V_xO_2$ with recently reported cathodes.

Sample	Specific capacity	Rate capacity retention	Capacity retention	Reference
MnO_2-BET//Zn	306 mAh g^{-1} at 0.1 A g^{-1}	105 mAh g^{-1} at 5.0 A g^{-1}	100% at 1.0 A g^{-1} (after 700 cycles); 95% at 5.0 A g^{-1} (after 8000 cycles)	[1]
CMC-MnO_2//Zn	324 mAh g^{-1} at 0.5A g^{-1}	237 mAh g^{-1} at 3 A g^{-1}	100% at 0.5 A g^{-1} (after 200 cycles) 86.2% at 1.5 A g^{-1} (after 1000 cycles)	[2]
NHMO //Zn	287.9 mAh g^{-1} at 0.1 A g^{-1}	99.4mAh g^{-1} at 6 A g^{-1}	96.5% at 0.2A g^{-1} (after 500 cycles) 90% at 6 A g^{-1} (after 13000 cycles)	[3]
H-MnO_2//Zn	260 mAh g^{-1} at 0.2 A g^{-1}	97 mAh g^{-1} at 3.8 A g^{-1}	98% at 0.4 A g^{-1} (after 100 cycles) 95% at 3.8 A g^{-1} (after 5000 cycles)	[4]
Ca/N-MnO_2//Zn	325 mAh g^{-1} at 0.3A g^{-1}	64.2 mAh g^{-1} at 3 A g^{-1}	70% at 1 A g^{-1} (after 200 cycles)	[5]

			70.4% at 3 A g^{-1} (after 1000 cycles)	
MnO_2//Te	177 mAh g^{-1} at 0.1 A g^{-1}	62 mAh g^{-1} at 5 A g^{-1}	76.5% at 1 A g^{-1} (after 5000 cycles)	[6]
MnO_2@AE PA	268 mAh g^{-1} at 0.2 A g^{-1}	84 mAh g^{-1} at 5 A g^{-1}	100% at 0.5 A g^{-1} (after 200 cycles) 97% at 1 A g^{-1} (after 1700 cycles)	[7]
T-MnO_2//Zn	398 mAh g^{-1} at 0.2 A g^{-1}	90 mAh g^{-1} at 1.5 A g^{-1}	100% at 1.0 A g^{-1} (after 1200 cycles)	[8]
δ-MnO_2@2-ML	309.5 mAh g^{-1} at 0.1 A g^{-1}	137.6mAh g^{-1} at 1.0A g^{-1}	80% at 1.0A g^{-1} (after 1350 cycles)	[9]
Bi-MnO_2//Zn	363 mAh g^{-1} at 0.1 A g^{-1}	103 mAh g^{-1} at 3.0 A g^{-1}	100% at 0.1 A g^{-1} (after 100 cycles) 93% at 1.0 A g^{-1} (after 10000 cycles)	[10]
MnO_2(O_d) //Zn	330.9 mAh g^{-1} at 0.1 A g^{-1}	225 mAh g^{-1} at 2.0 A g^{-1}	88.9% at 1 A g^{-1} (after 800 cycles)	[11]
WO3/WC|| MnO_2/graphite	69 mAh g^{-1} at 0.1 A g^{-1}	21 mAh g^{-1} at5.0 A g^{-1}	100% at 1.0 A g^{-1} (after 10000 cycles)	[12]
NHVO@Ti_3	498.4 mAh g^{-1}	98.2 mAh g^{-1} at	92.1% at 2.0 A g^{-1} (after	[13]

C_2T_x//ZnMn$_2O_4$	at 0.1 A g^{-1}	2.0 A g^{-1}	6000 cycles)	
p-$MoSe_2$||Znx NVPF	84.8 mAh g^{-1} at 0.04 A g^{-1}	28.1 mAh g^{-1} at 0.04 A g^{-1}	71.9 % at 0.015A g^{-1} (after 160 cycles) 79.9% at 0.2A g^{-1} (after 5000 cycles)	[14]
AgNWA@ Zn//α-MnO2	240.6 mAh g^{-1} at 0.1 A g^{-1}	90.0 mAh g^{-1} at 10.0 A g^{-1}	94.4% at 5.0A g^{-1} (after 1500 cycles)	[15]
Se-MnO_2//Zn	368 mAh g^{-1} at 0.1 A g^{-1}	125 mAh g^{-1} at 0.1 A g^{-1}	100% at 0.1A g^{-1} (after 100 cycles) 71% at 3 A g^{-1} (after 5000 cycles)	[16]
K-MnO_2//Zn	285 mAh g^{-1} at 0.2 C	211.8 mAh g^{-1} at 4 C	80.1% at 1 C (after 100 cycles)	[17]
Mo-MnO_2//Zn	270 mAh g^{-1} at 0.1 A g^{-1}	90 mAh g^{-1} at 2 A g^{-1}	92.6% at 0.1A g^{-1} (after 100 cycles) 80.1% at 1 A g^{-1} (after 16000cycles)	[18]
Ag-MnO_2//Zn	306 mAh g^{-1} at 0.1 A g^{-1}	160 mAh g^{-1} at 2 A g^{-1}	75% at 0.1 A g^{-1} (after 75 cycles) 50% at 1 A g^{-1} (after 800	[19]

			cycles)	
Mg-MnO_2//Zn	600 mAh g^{-1} at 1 C	260 mAh g^{-1} at 5 C	77.2% at 1C (after 700 cycles) 36% at 5C (after 640 cycles)	[20]
$Mn_{1-x}V_xO_2$//Te@C	323.7mAh g^{-1} at 0.1 A g^{-1}	120.5mAh g^{-1} at 3A g^{-1}	92.93% at 0.5 A g^{-1} (after 1000 cycles) 94.08% at 0.5 A g^{-1} (after 5000 cycles)	This work
$Mn_{1-x}V_xO_2$//Zn	406.9 mAh g^{-1} at 0.1 A g^{-1}	119.2mAh g^{-1} at 3A g^{-1}	97.04% at 0.5 A g^{-1} (after 200 cycles) 74.34% at 3 A g^{-1} (after 3000 cycles)	This work

References

1. A. Zhang, X. Yin, I. Saadoune, Y. Wei, Y. Wang, *Small*, 2024, **20**, 2402811.

2.X. Zhang, X. Ma, H. Bi, Y. Zhang, P. Mi, F. Liu, X. Jin, Y. Chen, K. Zhang, J. Wang, *Adv. Funct. Mater.*, 2025, 35, 2411990.

3. Z. Xu, J. Wang, W. Zhang, Z. Shi, Y. Feng, C. Liu, H. Fu, Z. Yong, Q. Li, *J. Mater. Chem. A*, 2024, 12, 25491-25503

4. M. Li, C. Liu, J. Meng, P. Hei, Y. Sai, W. Li, J. Wang, W. Cui, Y. Song, X. X. Liu, *Adv. Funct. Mater.*, 2024, 34, 2405659.

5. Y. Xu, G. Zhang, X. Wang, J. Zhang, H. Wen, D. Wang, Y. Yuan, Q. Jiang, H. Qian, Y. Xi, *Adv. Funct. Mater.*, 2025, **35**,2500137.

6. Z. Chen, C. Li, Q. Yang, D. Wang, X. Li, Z. Huang, G. Liang, A. Chen, C. Zhi, *Adv. Mater.*, 2021, **33**, 2105426.

7. X. Xiao, L. Zhang, W. Xin, M. Yang, Y. Geng, M. Niu, H. Zhang, Z. Zhu, *Small,* 2024, **20**, 2309271

8. K. Shin, Y. Pei, X. Zhou, Q. Chen, P. Kidkhunthod, Y. Zheng, X. Guo, S. Tunmee, Q. Zhang, Y. Tang, *Adv. Mater.*, 2025, 37, 2413645.

9. Y. Ding, K. Zhu, H. Jin, W. Gao, B. Wang, S. Bian, R. He, J. Wang, H. Yang, K. Denis, *Carbon Energy*, 2025, **7**,e70014

10. Y. Ma, M. Xu, R. Liu, H. Xiao, Y. Liu, X. Wang, Y. Huang, G. Yuan, *Energy Storage Mater.*, 2022, **48**, 212

11. J. Zheng, C. Qin, C. Chen, C. Zhang, P. Shi, X. Chen, Y. Gan, J. Li, J. Yao, X. Liu, *J. Mater. Chem. A*, 2023, **11**, 24311.

12. J. Cao, D. Zhang, Y. Yue, X. Wang, A. Srikhaow, C. Sriprachuabwong, A. Tuantranont, X. Zhang, Z. S. Wu, J. Qin, *Chem. Eng. J.*, 2021, **426**, 131893.

13. X. Wang, Y. Wang, Y. Jiang, X. Li, Y. Liu, H. Xiao, Y. Ma, Y. y. Huang, G. Yuan, Tailoring *Adv. Funct. Mater.*, 2021, **31**, 2103210.

14. Z. Lv, Y. Kang, R. Tang, J. Yang, G. Chen, Y. Hu, P. Lin, H. Yang, Q. Wu, M. Zhang, *Electron*, 2023, **1**, e5.

15. W. Ling, Q. Yang, F. Mo, H. Lei, J. Wang, Y. Jiao, Y. Qiu, T. Chen, Y. Huang, *Energy Storage Mater.*, 2022, **51**, 453.

16. J. J. Ye, P. H. Li, Z. Hou, W. Zhang, W. Zhu, S. Jin, H. Ji, S *Angew. Chem.*, 2024, **136**, e202410900.

17. Y. Li, X. Liu, T. Ji, M. Zhang, X. Yan, M. Yao, D. Sheng, S. Li, P. Ren, Z. Shen, *Chin. Chem. Lett.*, 2025, **36**, 109551.

18. Y. Liu, K. Wang, X. Yang, J. Liu, X.-X. Liu, X. Sun, *ACS nano*, 2023, **17**, 14792.

19. F. W. Fenta, B. W. Olbasa, M.-C. Tsai, N. T. Temesgen, W.-H. Huang, T. M. Tekaligne, Y. Nikodimos, S.-h. Wu, W.-N. Su, H. Dai, *J. Power Sources,* 2022, **548**, 232010.

20. Q. Li, C. Wang, Y. Zhu, W. Du, W. Liu, M. Yao, Y. Wang, Y. Qian, S. Feng, *Chem.Eng.J.*, 2024, **485**, 150077.